Electronic Supplementary Material (ESI) for Journal of Materials Chemistry A.

SUPPORTING INFORMATION

Effect of sulfur-containing additives on the formation of solid-electrolyte interphase evaluated by in-situ AFM and ex-situ characterizations

Lingpiao Lin, Kai Yang, Rui Tan, Maofan Li, Shaojie Fu, Tongchao Liu, Haibiao Chen*and Feng Pan*

School of Advanced Materials, Peking University, Shenzhen Graduate School, Shenzhen 518055, People's Republic of China

*E-mail: chenhb@pkusz.edu.cn; panfeng@pkusz.edu.cn

Section 1. Diagram of the *in-situ* AFM equipment and the test method.

Fig. S1. The cross-sectional view of the liquid cell with electrochemical connections.

The evolution of the morphology the HOPG surface was observed and the cyclic voltammetry was performed at the same time. Fresh surface of the HOPG electrode was ready before every *in-situ* AFM experiment. The liquid cell was covering the HOPG electrode, and a Li wire as the counter electrode was set inside the groove of the cell. The electrolyte was sealed with an O-ring and the AFM tip was placed under the cell. The electrodes were connected to an electrochemical workstation.

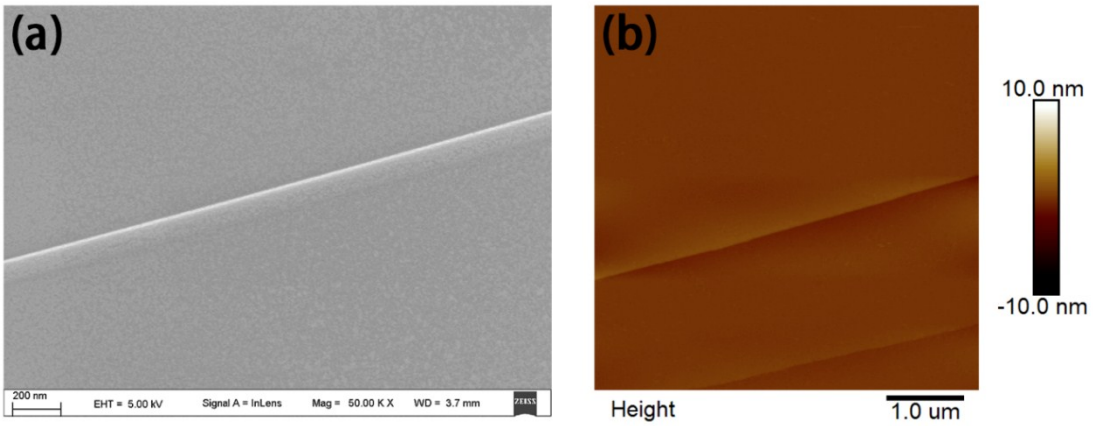

Fig. S2 (a) SEM image and (b) AFM image of fresh HOPG surface cleaved with adhesive tape.

Section 2. *in-situ* AFM test on HOPG in regular electrolyte without additives

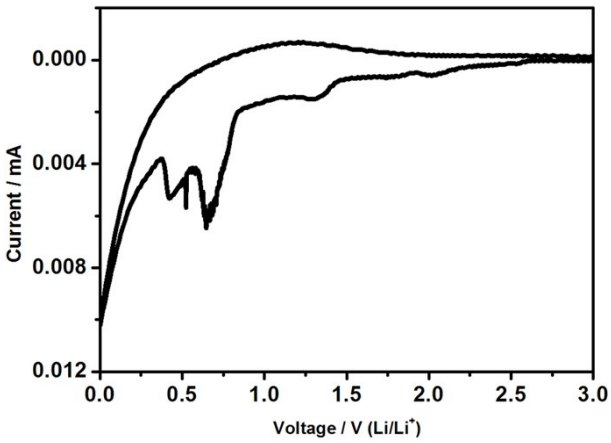

Fig. S3 CV curve of the freshly cleaved HOPG electrode in 1.0 M $LiPF_6$/EC/DMC at a scan rate of 2 mV s^{-1}.

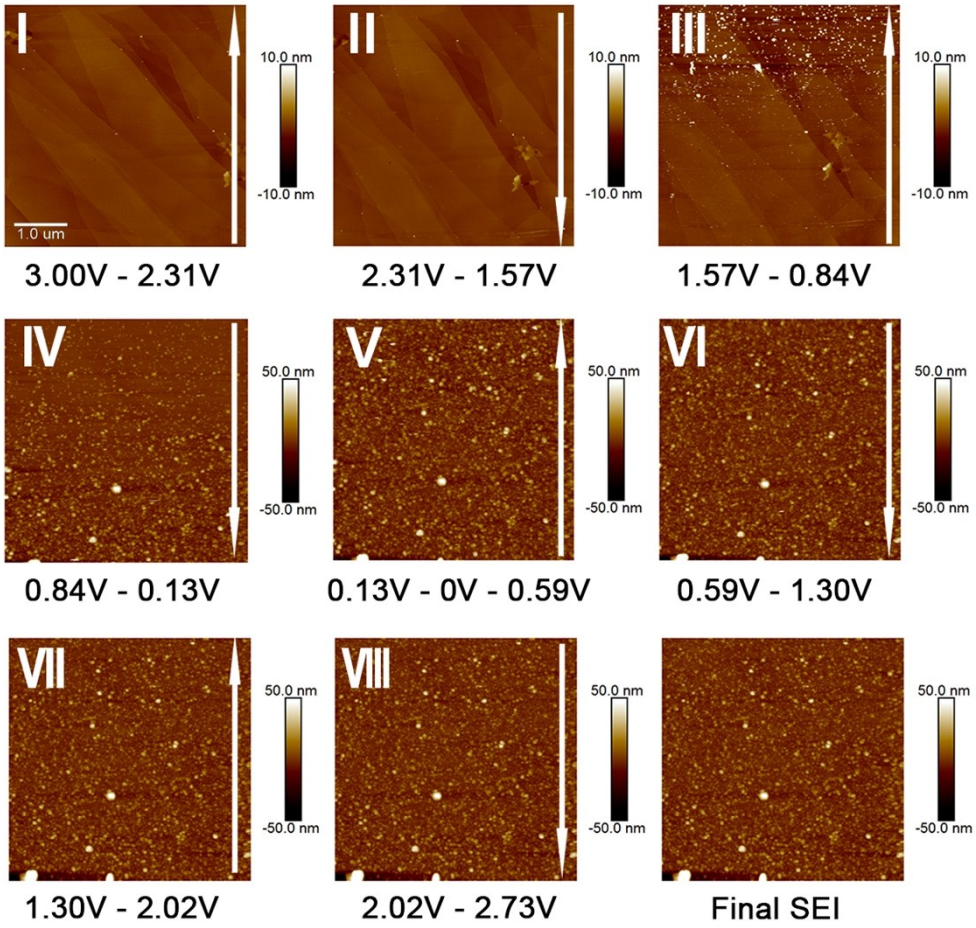

Fig. S4 Corresponding *in-situ* AFM images showing the evolution of the SEI on HOPG. The arrows indicate the scanning direction.

Section 3. *in-situ* AFM test on HOPG in electrolyte containing ES

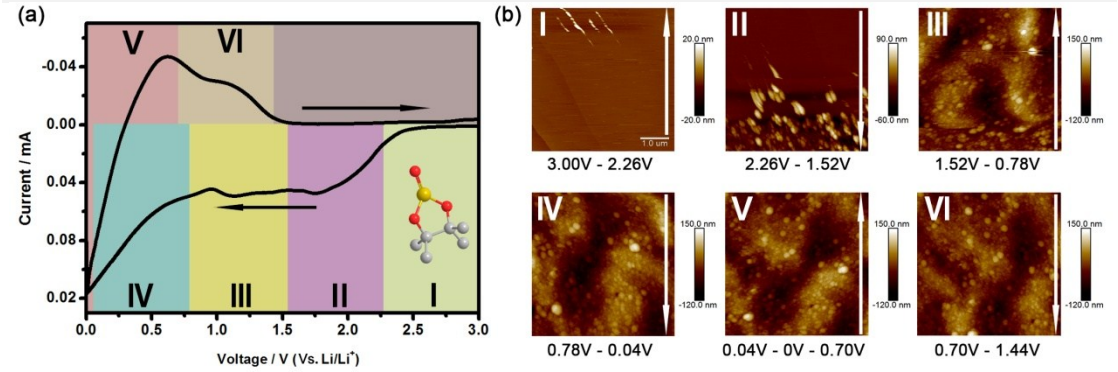

Fig. S5 (a) CV curve of the freshly cleaved HOPG electrode in 1.0 M $LiPF_6$/EC/DMC with 1% ES at a scan rate of 2 mV s^{-1}. Labelled regions I-VI indicate the range of potentials where every AFM image was collected. Arrows indicate the scanning direction is 3.0-0.0-3.0 V. (b) (I-VI) Corresponding in-situ AFM images showing the evolution of the SEI on HOPG. The arrows indicate the scanning direction.

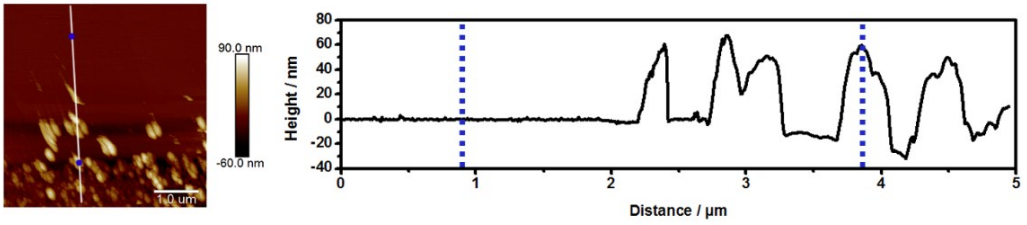

Pair	Horizontal Distance	Vertical Distance	Angle
1	2.300 (µm)	50.709 (nm)	1.263 (°)

Fig. S6 The height measurement of the initial SEI formation (potential range: 2.26 V – 1.52 V). The blue dots in the image and corresponding dashed lines in the height profile label the measuring sites of the basal plane and an SEI particle, respectively, which shows the vertical height of the particle was 50.709 nm.

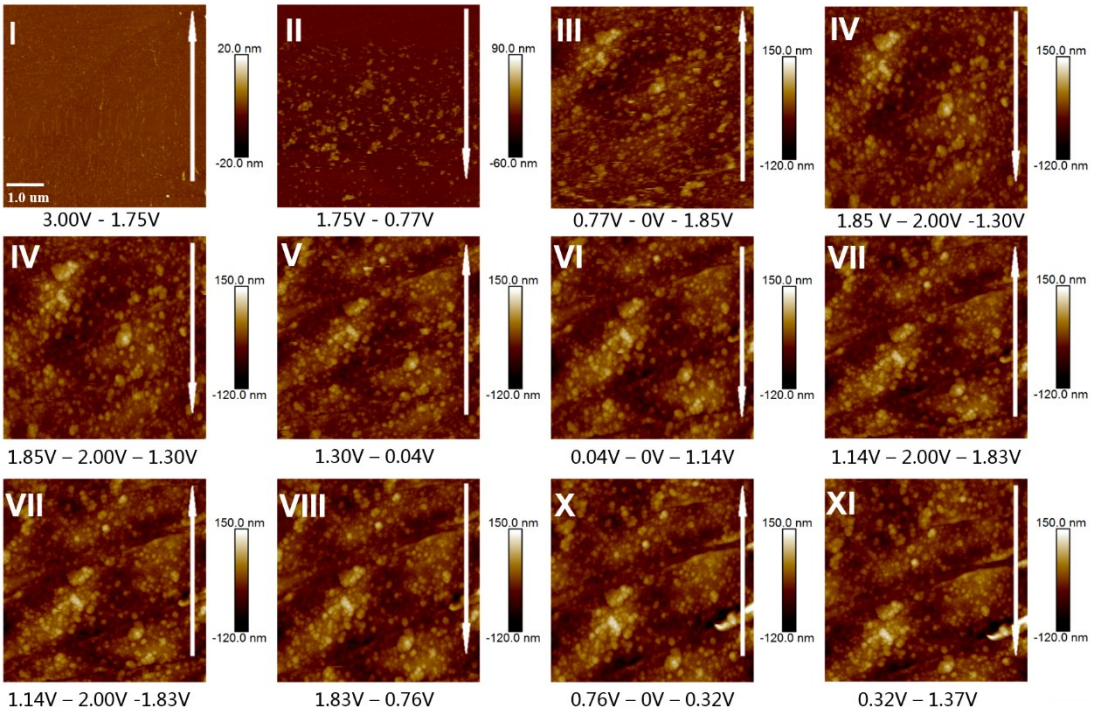

Fig. S7 AFM test on HOPG in 1.0 M $LiPF_6$/EC/DMC with 1% ES at a scan rate of 2 mV s^{-1} during initial three cycles. Labelled regions I-VI indicate AFM images collected during the first cycle. IV-VII Corresponding in-situ AFM images during the second cycle. VII-XI Corresponding in-situ AFM images during the third cycle. The arrows indicate the scanning direction.

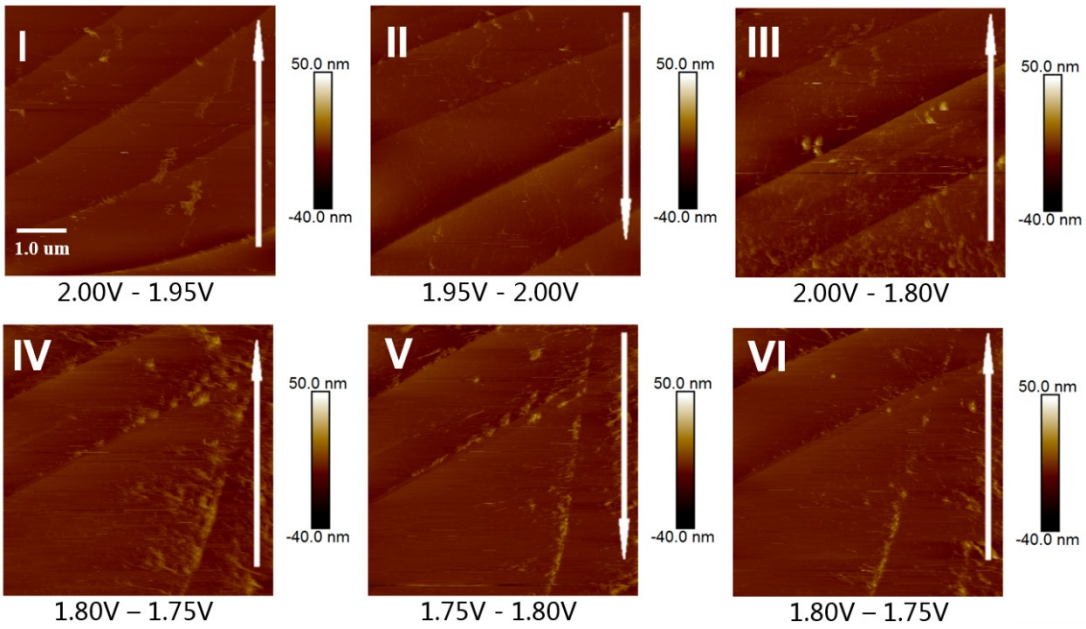

Fig. S8 Quasi-static AFM test on HOPG in 1.0 M $LiPF_6$/EC/DMC with 1% ES at a scan rate of 0.5 mV s^{-1} above the ES reduction potential. Labelled regions I-II indicate AFM images collected between 2.00V–1.95V. Labelled regions III indicate AFM

images collected near 1.80V which is the reduction potential of ES. Labelled regions IV- VI indicate AFM images collected during 1.80V-1.75V for several cycles. The arrows indicate the scanning direction.

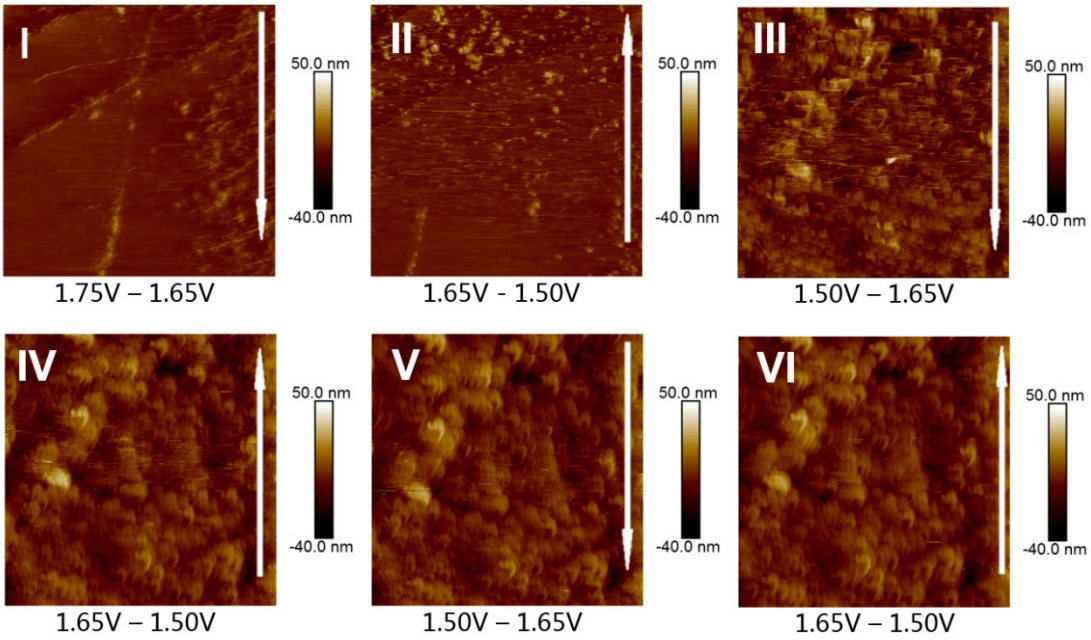

Fig. S9 Quasi-static AFM test on HOPG in 1.0 M $LiPF_6$/EC/DMC with 1% ES at a scan rate of 0.5 mV s^{-1} below the ES reduction potential. Labelled regions I indicate AFM images collected between 1.75V–1.65V. Labelled regions II-VI indicate AFM images collected between 1.65V-1.50V for several cycles. The arrows indicate the scanning direction.

Section 4. *in-situ* AFM test on HOPG in electrolyte containing PES

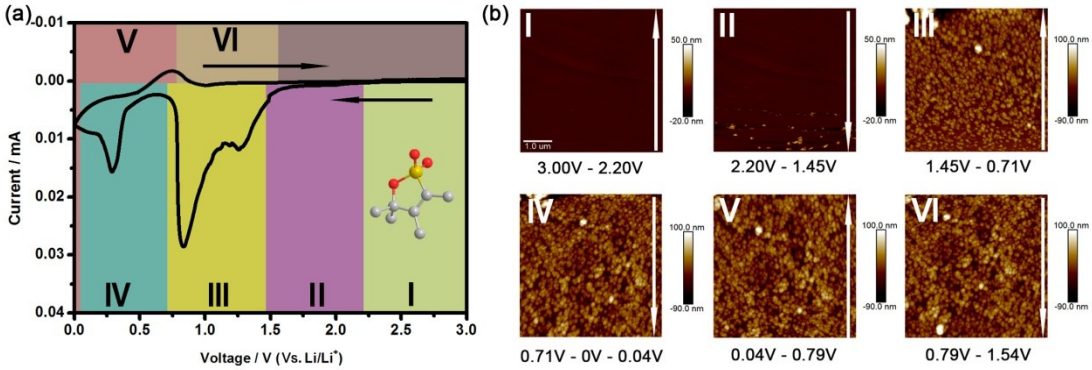

Fig. S10 (a) CV curve of the freshly cleaved HOPG electrode in 1.0 M $LiPF_6$/EC/DMC with 1% PES at a scan rate of 2 mV s^{-1}. Labelled regions I-VI indicate the range of potentials where every AFM image was collected. Arrows indicate the scanning

direction is 3.0-0.0-3.0 V. (b) (I-VI) Corresponding in-situ AFM images showing the evolution of the SEI on HOPG. The arrows indicate the scanning direction.

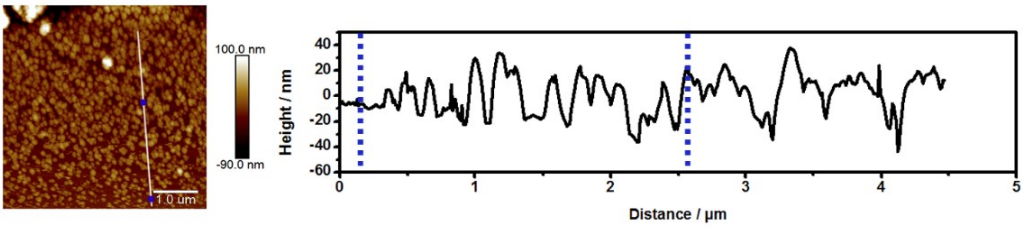

Pair	Horizontal Distance	Vertical Distance	Angle
1	2.400 (µm)	30.081 (nm)	0.718 (°)

Fig. S11 The height measurement of the initial SEI formation (potential range: 1.45 V – 0.71 V). The blue dots in the image and corresponding dashed lines in the height profile label the measuring sites of the basal plane and an SEI particle, respectively, which shows the vertical height of the particle was 30.081 nm.

Section 5. The electrochemical performance of coin cells

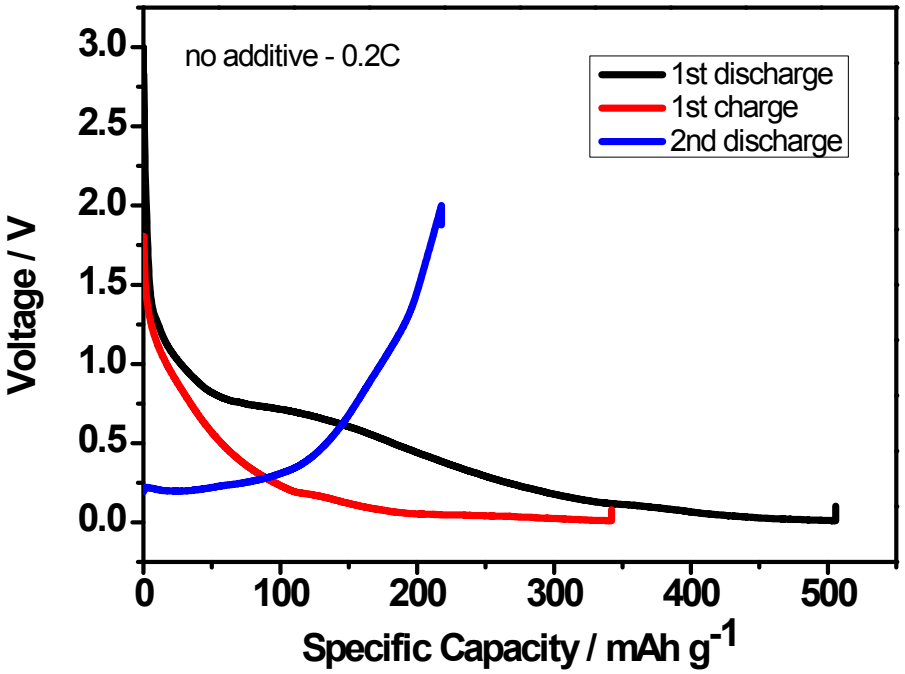
no additive - 0.2C
1st discharge
1st charge
2nd discharge
Voltage / V
Specific Capacity / mAh g-1
3.0
2.5
2.0
1.5
1.0
0.5
0.0
0
100
200
300
400
500

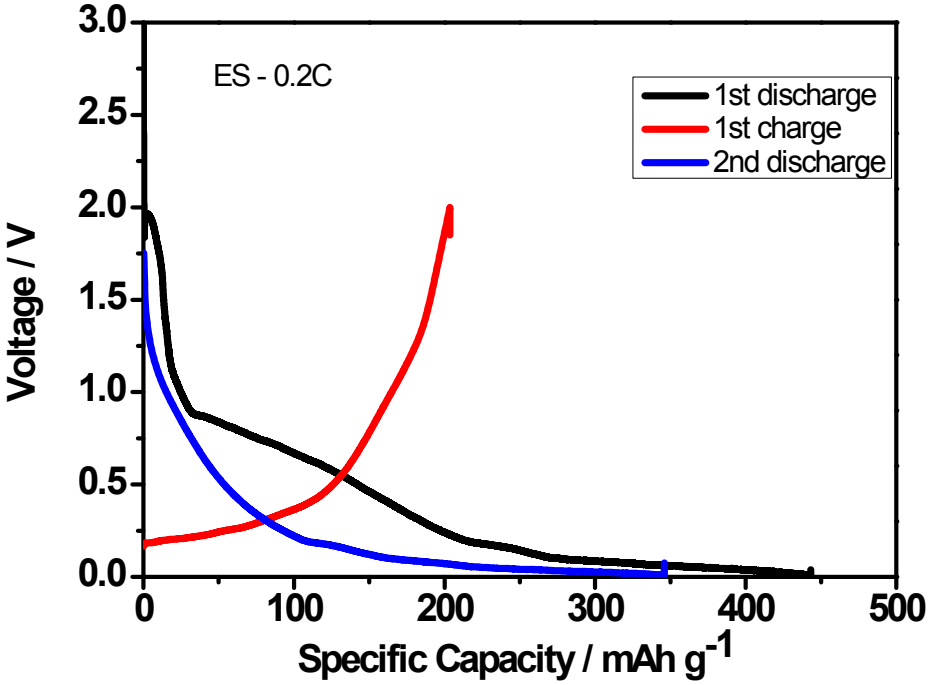
ES - 0.2C
1st discharge
1st charge
2nd discharge
Voltage / V
Specific Capacity / mAh g-1
3.0
2.5
2.0
1.5
1.0
0.5
0.0
0
100
200
300
400
500

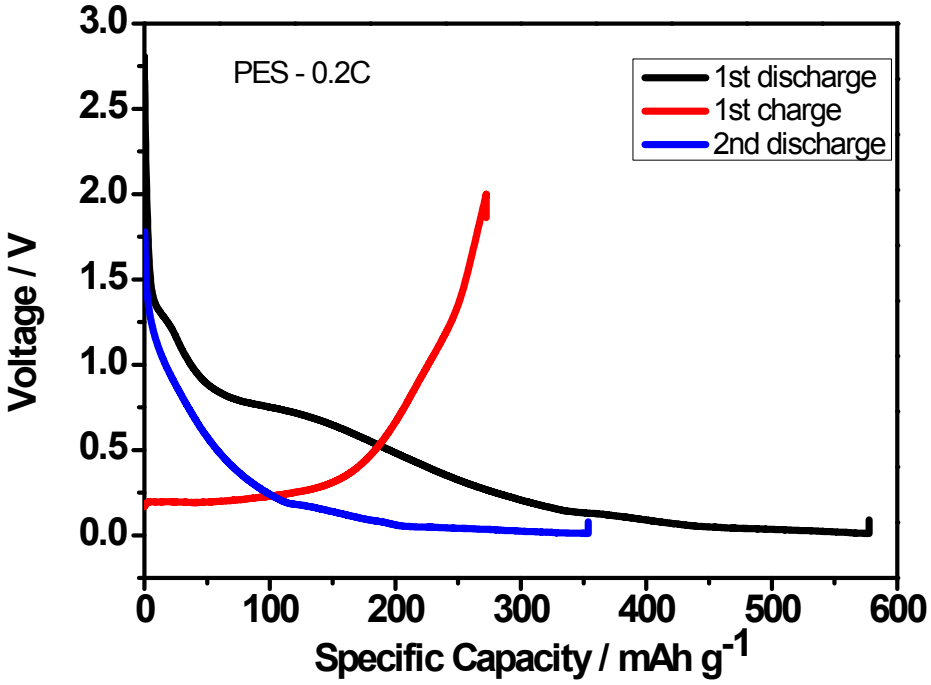

Fig. S12 The charge and discharge curves of graphite in different electrolytes at 0.2 C rate.

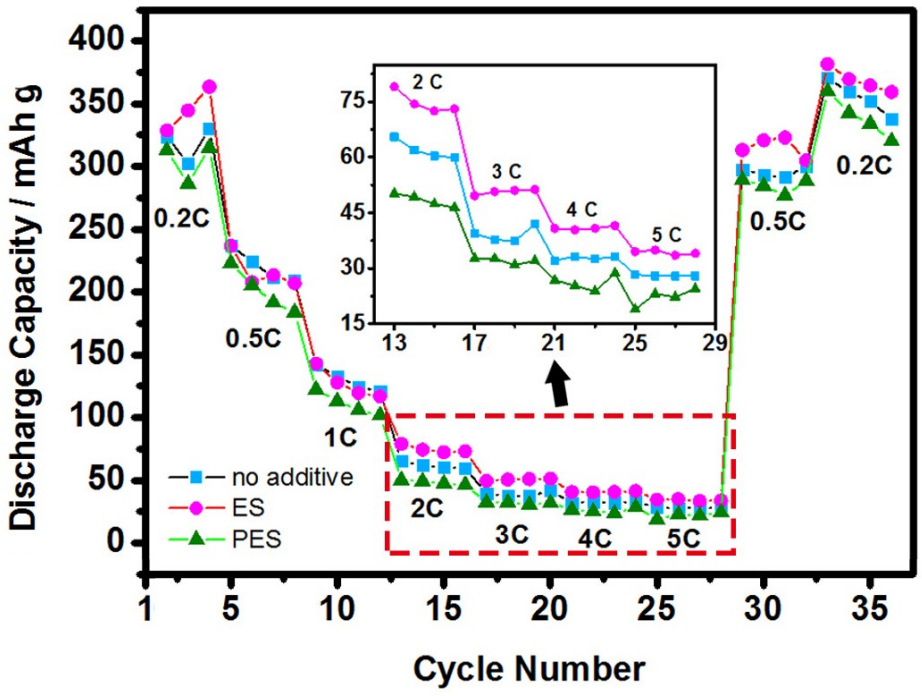

Fig. S13 Rate performance of coin cells with three types of electrolytes.

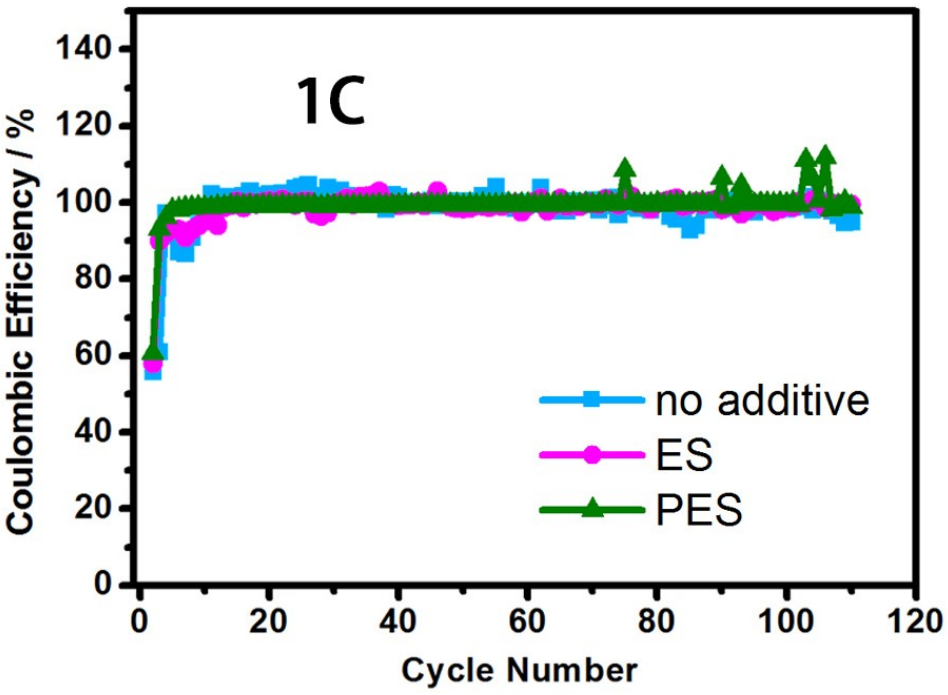

Fig. S14 The cycling stability of coin cells with three different types of electrolytes at 1 C rate. All coin cells were activated with 0.2C for two cycles before other rate test.

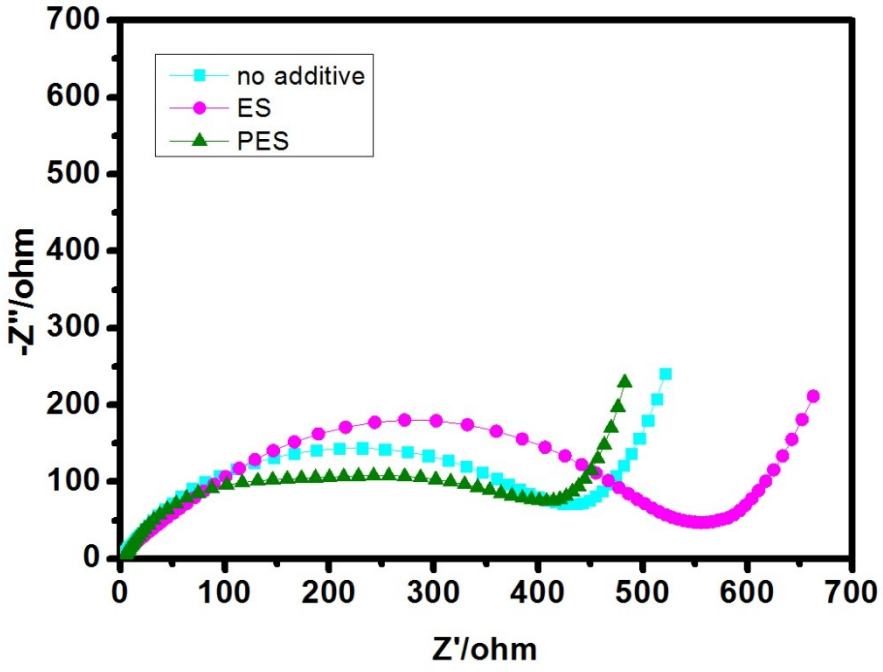

Fig. S15 The Nyquist plots of fresh coin cells before charge-discharge.

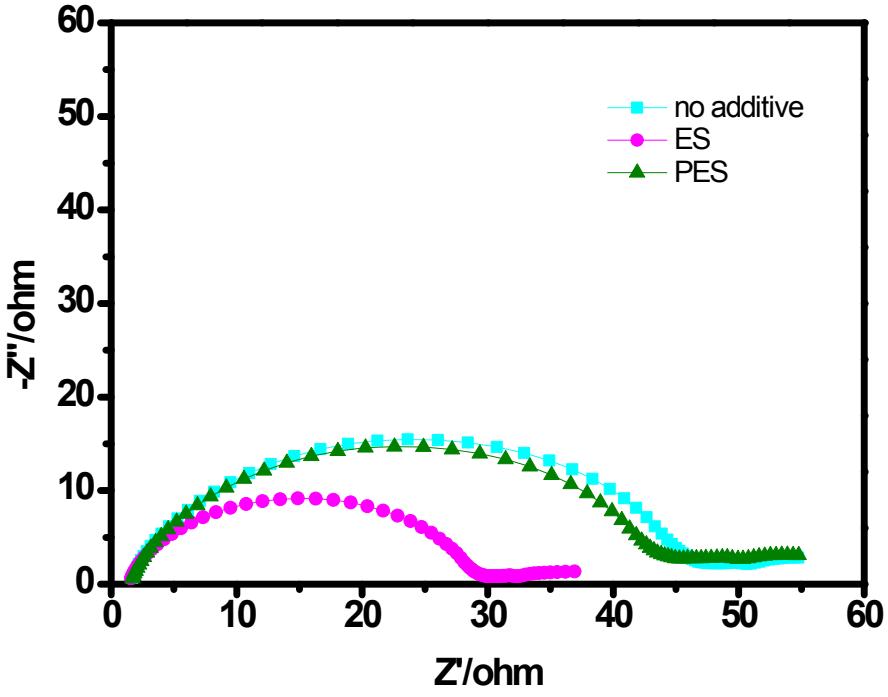

Fig. S16 The Nyquist plots of Li/Li coin cell after several CV cycles until stable.

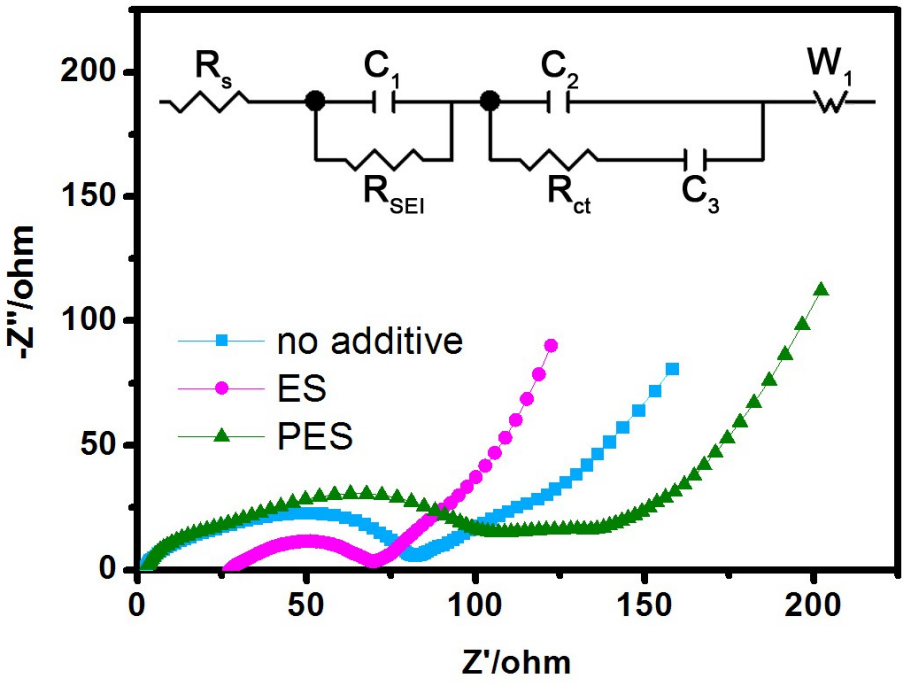

Fig. S17 Nyquist plots and equivalent circuit of the coin cells with three types of electrolytes after 300 cycle at 5 C rate.

Section 6. Images of the electrodes from different coin cells.

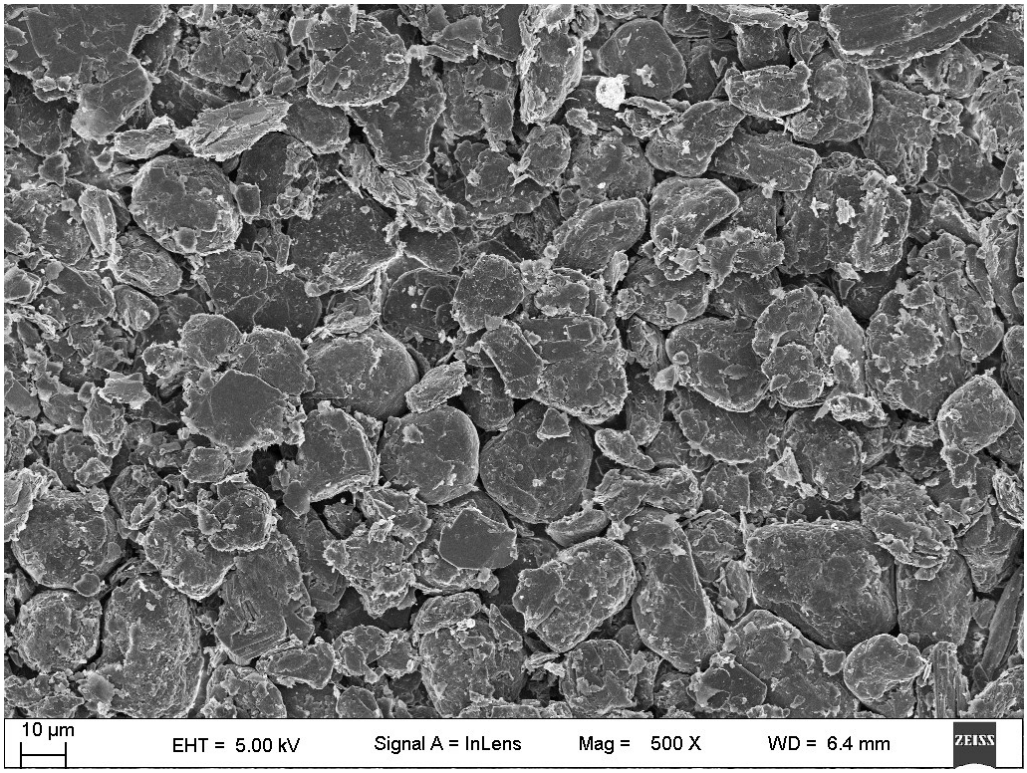

Fig. S18 SEM image of natural graphite.

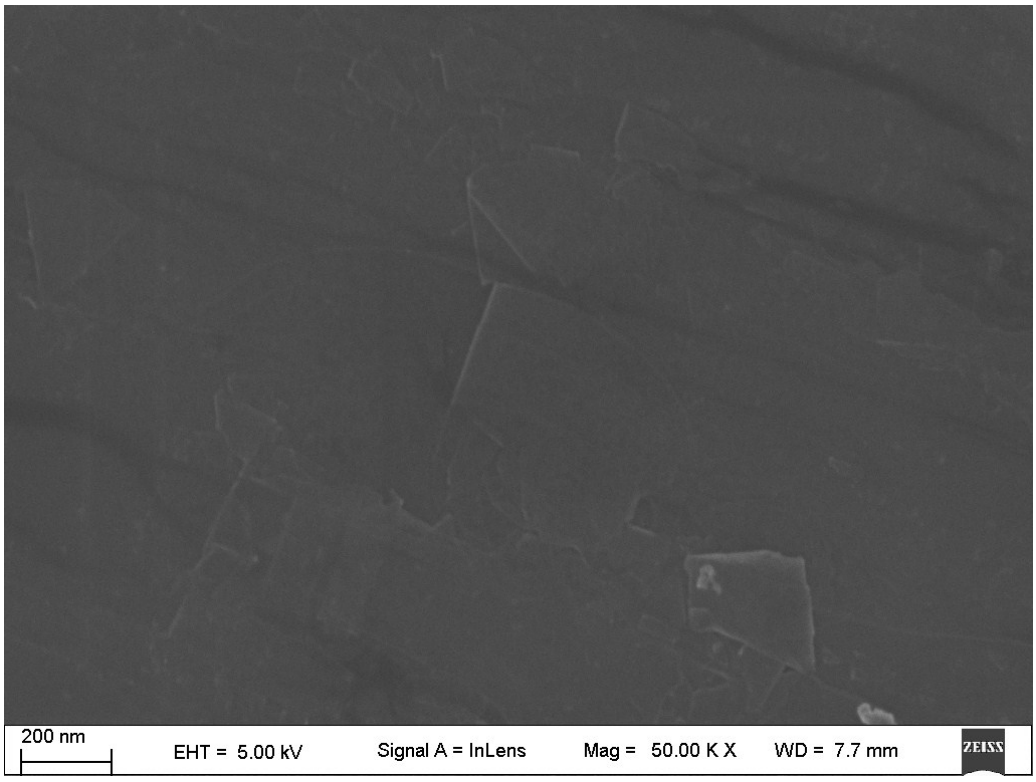

Fig. S19 SEM image of the graphite electrode in a fresh coin cell.

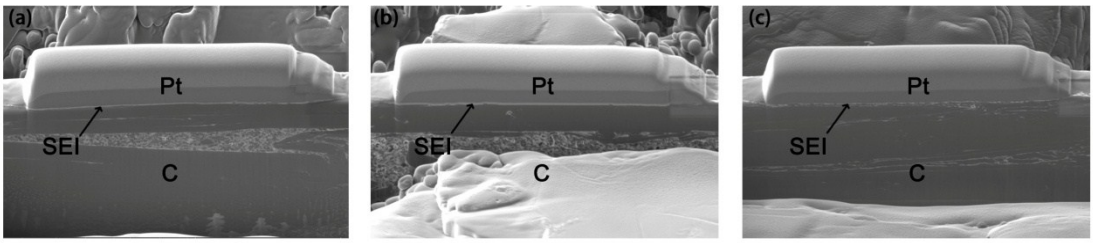

Fig. S20 FIB images of the cross-section of the SEI layer from (a) regular electrolyte, (b) ES-containing electrolyte, and (c) PES-containing electrolyte.

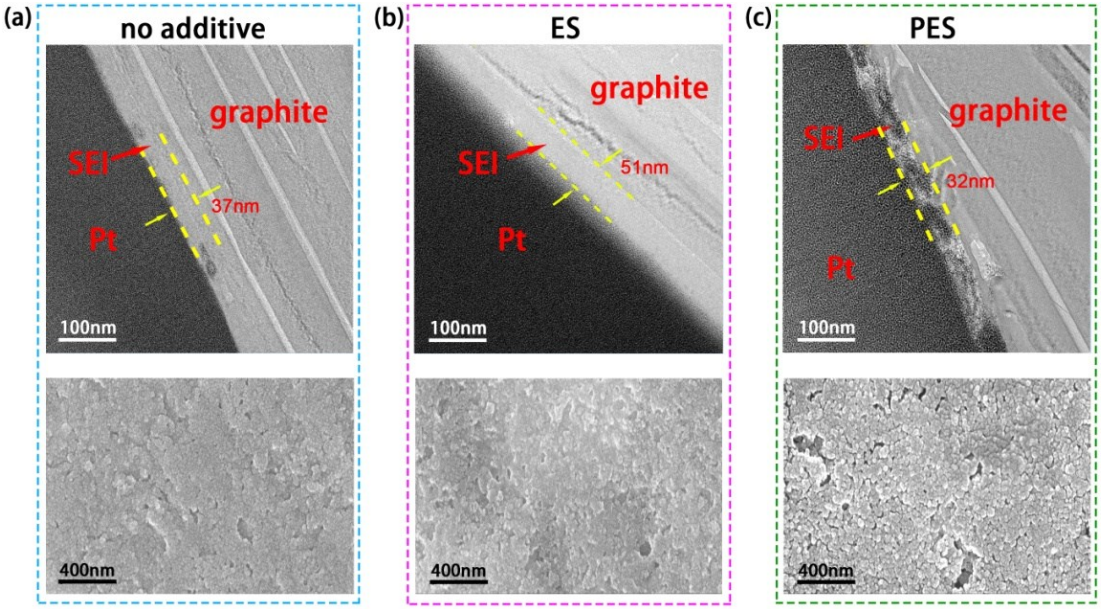

Fig. S21 TEM and SEM image of the SEI layer in (a) regular electrolyte (b) ES-containing electrolyte, and (c) PES-containing electrolyte, after tested at 5 C rate for 50 cycles.